Development of a high finesse cavity for portable clock applications

Rishabh Pal
Department of Physics
Indian Institute of Technology Tirupati
Tirupati, India
ph22d502@iittp.ac.in

Anup Basak
Department of Mechanical Engineering
Indian Institute of Technology Tirupati
Tirupati, India
abasak@iitp.ac.in

Arijit Sharma
Department of Physics
Indian Institute of Technology Tirupati
Tirupati, India
arijit@iittp.ac.in

***Abstract*—Portable optical atomic clocks based on dipole-forbidden narrow linewidth optical transitions have shown significant promise for next-generation applications in positioning, navigation, and timing (PNT) domain. Such optical clocks are poised to revolutionize PNT applications in communication, deep space missions, VLBI (very long baseline interferometry), and geodetic measurements due to their exceptional frequency stability. Achieving this stability involves the use of narrow linewidth lasers, stabilized to ultra-stable high finesse optical cavities using the Pound-Drever-Hall (PDH) technique of laser frequency stabilization. Stability in frequency is directly determined by the stability in optical length of the high finesse cavity. However, the stability in optical length of these cavities is limited by fundamental thermal noise and external noise sources such as vibrations, temperature fluctuations, acoustic noise, etc. Finite Element Analysis (FEA) plays a pivotal role in optimizing cavity design by exploring various configurations, materials, and mounting strategies to minimize these instabilities. This article examines the influence of the fundamental thermal noise floor on stability, considering factors such as cavity length and mirror curvature. It also presents and discusses methodologies using FEA to identify the optimal mounting positions to minimize the acceleration sensitivity and deformation due to self-weight.**

***Index Terms*—high-finesse optical cavity, portable all-optical clock, finite element analysis, airy points**

I. Introduction

Portable optical atomic clocks have emerged as promising candidates for next-generation applications in communication, positioning, navigation, timing etc [1], [2]. These clocks have the potential to form a resilient PNT system. Such clocks are based on narrow linewidth (Δv) dipole-forbidden optical transitions (known as a clock transition, v) and thus have better stability compared to their microwave counterparts owing to their higher quality factor ($\mathrm{Q} = \Delta v/v$). For coherent probing of an optical clock transition, an ultra-stable, narrow linewidth (Hz or sub-Hz) laser (clock laser) is an indispensable tool to realise this objective. Such narrow linewidth laser also serves as a local oscillator and determines the short-term stability ($1\mathrm{msec}$ $10\mathrm{sec}$) in an optical clock framework.

To realize a clock laser, it is frequency stabilized to one of the resonance peaks of an ultrastable high-finesse Fabry-Perot cavity, using the Pound-Drever-Hall (PDH) technique of laser frequency stabilization. In the PDH technique, the fractional stability in length ($\Delta\mathrm{L}/\mathrm{L}$, L and $\Delta\mathrm{L}$ represent the length and displacement in length of the cavity respectively) of an ultra-stable Fabry-Perot (FP) cavity is transferred to the clock laser (oscillator) according to equation $\Delta\mathrm{L}/\mathrm{L} = -\Delta v/v$ [3]. However, the stability in the optical length of a FP cavity is primarily limited by two factors: one is the fundamental thermal noise floor, and the other one is the external noises such as deformation due to self-weight, vibrational noise, thermal fluctuations, acoustic noises, etc. The aforementioned issues posed formidable challenges to develop an ultra-stable high finesse optical cavity. As a result, quantifying instabilities originating from different noise sources becomes crucial for optimizing the design of a high-finesse optical cavity. Finite Element Analysis (FEA) techniques play a pivotal role in optimizing cavity design by exploring configurations, materials, and mounting strategies to minimize these instabilities [4]–[7]. Quantitative analysis using FEA gives an upper hand in aiding non-destructive evaluation of such optical cavity design to ensure exceptional performance. Despite these studies, imperfections in the manufacturing and mounting processes may result in a non-zero vibrational sensitivity. In this regard, FEA calculations may enable the user to determine the appropriate machining tolerances that meet the desired frequency stability.

In this article, we shall briefly discuss how the fundamental thermal noise floor puts an ultimate limit on the stability and how it is influenced by the radius of curvature (ROC) of mirrors and cavity length. We present a methodology to identify the mounting points (Airy points) for which deformation in optical length due to self-weight is minimized for the cavity.

II. Fundamental thermal noise floor

Fundamental thermal noise primarily puts a limit on the stability of an ultra-stable cavity. This noise arises from the various components of the cavity, leading to fluctuations in the optical length of the cavity. Due to these noises, length fluctuation power spectral density denoted by $S_L(f)$, considering all contributing components, can be described as follows [8]:

$$\begin{aligned} S_L(f) =& \frac{4K_B T}{\pi f F_0^2}(U_{\mathrm{SP}}\alpha_{\mathrm{SP}} + U_{\mathrm{MS1}}\alpha_{\mathrm{MS1}} \\ &+ U_{\mathrm{MS2}}\alpha_{\mathrm{MS2}} + U_{\mathrm{MC1}}\alpha_{\mathrm{MC1}} \\ &+ U_{\mathrm{MC2}}\alpha_{\mathrm{MC2}}) \end{aligned} \tag{1}$$

Here, U signifies maximum elastic strain energy corresponding to maximum deformation of a test mass subjected

to a periodic force F of frequency f, and α represents the mechanical loss angle. K_B and T represents the Boltzmann's constant and the operating temperature. The abbreviations SP, MS1, MS2, MC1, and MC2 represent spacer, input mirror substrate, end mirror substrate, input mirror coating and end mirror coating, respectively. If mirror substrates and coatings are identical, then the power spectral density given by (1) is reduced to

$$\begin{aligned} S_L(f) &= \frac{4K_BT}{\pi f F_0^2}\left(U_{SP}\alpha_{SP} + 2U_{MS}\alpha_{MS} + 2U_{MC}\alpha_{MC}\right) \\ &= \left(S_{SP} + 2S_{MS} + 2S_{MC}\right) \end{aligned} \tag{2}$$

Here, S_{MS}, S_{MC}, S_{SP} depicts power spectral density due to length fluctuation originating from mirror substrate, coating, and spacer, respectively. The contributions from different parts are given by the following reported formulae [4]

$$S_{SP}(f) = \frac{4K_BT}{\pi f}\frac{L}{2\pi Y_{SP}\left(R_{SP}^2 - r_{SP}^2\right)}\alpha_{SP} \tag{3}$$

$$\mathrm{S_{MS}} = \frac{4\ \mathrm{K_B T}}{2\pi \mathrm{f}}\frac{1-\sigma_{\mathrm{MS}}^2}{\sqrt{\pi}\mathrm{Y_{MS}}\omega}\alpha_{\mathrm{MS}} \tag{4}$$

$$\mathrm{S_{MC}} = \frac{4\ \mathrm{K_B T}}{2\pi \mathrm{f}}\frac{2\left(1+\sigma_{\mathrm{Ms}}\right)\left(1-2\sigma_{\mathrm{MS}}\right)\mathrm{d_{MC}}}{\pi \mathrm{Y_{MS}}\omega^2}\alpha_{\mathrm{MC}} \tag{5}$$

$\mathrm{R_{SP}}$ and $\mathrm{r_{SP}}$ are the outer and inner (bore) radii of a cylindrical spacer of average length L, respectively. $\mathrm{Y_{MS}}$ and σ_{MS} denotes the Young's modulus and Poisson's ratio of the mirror substrate respectively, and d_{MC} is the thickness of mirror coating. The loss angle of the mirror substrate, mirror coating and spacer are indicated by α_{MS}, α_{MC} and α_{SP} respectively, and ω is the beam diameter at the mirror surfaces.

Instability of fractional frequency in time domain is given by Allan deviation, $\sigma_y(\tau)$. Since in (3),(4),(5) the thermal noise from all three contributions behaves as $1/f$, the resulting Allan deviation will be constant in time, given as [4],

$$\sigma_y(\tau) = \sigma_y = \sqrt{2\ln(2)S_y(f)f} \tag{6}$$

Fractional frequency instability due to spacer as indicated by (3) scales as $\frac{1}{\sqrt{L}}$ suggesting longer cavity spacers for lower thermal noise, but at the expense of vibrational stability. Consequently, a shorter spacer length restricts the stability

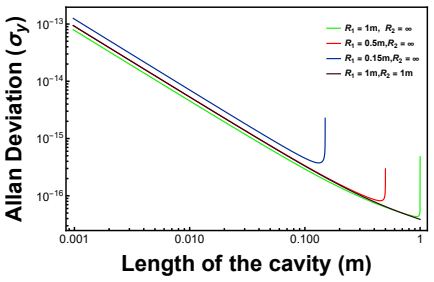

Fig. 1. Impact of cavity length and mirror curvatures on Allan Deviation (as a measure of instability)introduced due to fundamental thermal noise.

of portable cavities in achieving lower fundamental thermal noise in comparison to the stationary longer cavities [shown in Fig. 1]. Additionally, a smaller bore radius is advantageous due to the inverse relationship between noise spectral density and the cavity spacer face area. Noise contribution from mirror substrate and mirror coating scales as $\frac{1}{\omega}$ and $\frac{1}{\omega^2}$ respectively. Thus hemispherical ($R_1 = L$ or $2L, R_2 = \infty$ or vice versa, R_1 and R_2 are mirror radii of curvature) or near hemispherical cavity configuration would be more preferable to attain lower fundamental thermal noise level (as depicted in Fig. 1).

III. Design Optimization for Vibration-Insensitive Cavity using Finite Element Analysis

From the earlier discussion, it is evident that optical cavities exceeding 10 cm in length may achieve a fundamental thermal noise limit below 10^{-15} in terms of frequency instability. However, deformation due to self-weight and susceptibility to low-frequency environmental seismic and acoustic noises cause instantaneous fluctuations in the optical path length. This limits the attainment of the fundamental thermal noise floor in terms of stability. Consequently, stabilization against vibrational noise becomes essential for achieving ultrastable performance in such high-finesse optical cavities. This stability depends not only on the effective vibration isolation but also on the precise determination of mounting points, as well as the design and materials of the mounting structures and the contact points. According to Hooke's law, the self-weight of the cavity causes a change in its length. The deformation is primarily influenced by the position of the mounting structures. This effect can be mitigated by proper positioning of the mounting points, known as Airy points. Supporting the cavity at the Airy point can also significantly reduce the sensitivity of the cavity spacer to accelerations in all three directions.

The most significant vibrational noise that generates laser phase noise in an acoustically isolated environment occurs at low frequencies (below 100 Hz), generally coupling through the mounting supports. Therefore, it is sufficient to analyse the static case instead of a dynamical solution [5], where a gravitational acceleration can be applied uniformly to the whole body to investigate the deformation along the optical axis.

A. FEM Simulations

The instability in frequency of a laser stabilized to a FP cavity depends on the stability of optical length of the FP cavity, which can be depicted as the distance between the mirror centres. Rather than examining the deformation of the entire structure, it is more pertinent to focus on the deformation along the optical axis under static conditions. In this study, we consider a notched spacer (Fig. 2) supported at four points. Mirrors are made of fused silica (FS) and cavity spacer is constructed from ultra-low expansion (ULE) glass. The material properties are detailed in table I.

The coordinate system is defined with the Z-axis along the axial direction of the cavity, Y-axis along the vertical direction and X-axis along the radial direction (shown in

Fig.2). To investigate variation in the optical path length (i.e. displacement along the Z-axis), two deformation probes were set at the mirror centres (shown in Fig. 3). The change in the optical path can be given as

$$\Delta L = \Delta Z = \Delta Z_1 - \Delta Z_2 \tag{7}$$

where ΔZ_1 and ΔZ_2 are the displacement along the Z-axis at the probes located on mirror 1 and mirror 2, respectively. The simulation is performed using the commercially available FEA simulation platform ANSYS. The length of the cavity spacer is inspired by [6], and the design of the cavity is inspired by [4]. The parameters [7] used for the simulation are listed in table II.

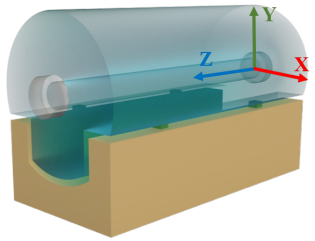

Fig. 2. schematic diagram of the cavity

TABLE I
MATERIAL PROPERTIES OF THE CAVITY

Cavity component	**Cavity spacer**	**Mirror**
Material	Ultra-low-expansion glass	Fused silica
Density (kg.m^{-3})	2210	2203
Young's modulus (GPa)	67.7	73.1
Poisson's ratio	0.17	0.17
Bulk modulus (GPa)	34.2	36.92

Fig. 3. Deformation probes at the centre of the mirrors. Probes on the right and left mirrors depict probe 1 and probe 2, respectively.

TABLE II
CAVITY PARAMETERS USED FOR SIMULATION

Cavity spacer length	12 cm
Cavity spacer diameter	6 cm
Bore diameter	1 cm
Mirror diameter	1.6 cm
ROC of mirrors	100 cm and ∞
Mirror thickness	5 mm
Cut-out area	25 mm^2

B. Constraints and Boundary Conditions

The support structure cutouts are square shaped and, for simplification of the problem, are treated as fixed supports to prevent translational and rotational motions. Gravitational acceleration ($g = 9.8$ m/s^2) is applied along the negative Y-axis. Mounting structures are symmetric about the centre of the cavity. As illustrated in Fig.4, δz and δx represent the measured distances of cavity support along the Z-axis and X-axis, respectively, from the centre of the cavity base plane.

C. Mesh Size and Study of Mesh Convergence

In the numerical calculation of deformation using the FEA method, one of the primary concerns is the determination of the optimum mesh element size, which significantly impacts the accuracy of the result. Generally, the smaller mesh element size leads to a higher number of mesh elements, thereby enhancing the accuracy of the calculations. However, this improvement in accuracy is at the expense of substantially increased computation time. As a result, without compromising accuracy, the determination of the optimum mesh size becomes one of the important factors in FEA-based numerical calculations.

We have kept the boundary conditions same as described in the previous section and investigated the deformation by varying the element size. Fig. 5 presents the relationship between deformation and the number of mesh elements, indicating that the deformation in optical length due to self-weight saturates around $10^6 - 10^7$ elements, which corresponds to an element size less than 0.2 mm.

Another important factor in achieving more accurate results is the selection of the mesh element order. In our calculations, we utilized quadratic mesh elements. While linear-order mesh elements offer computational cost benefits, they compromise the accuracy of deformation predictions. Conversely, quadratic-order mesh elements generally provide better accuracy in the FEA results.

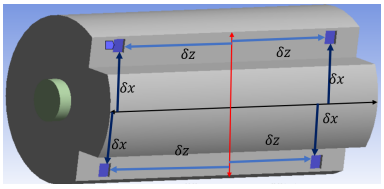

Fig. 4. Position of the mounting structures (blue-coloured surfaces), as measured from the centre of the cavity.

IV. RESULT AND DISCUSSIONS:

To identify optimal mounting positions, the support structure positions were varied along the Z and X directions, and the resulting displacement along the optical axis was calculated. When the cavity support structures are positioned near the end faces, there is a significant elongation in optical length due to the increased downward force at the central portion, resulting in a positive ΔL. Conversely, if the support positions are too far from the end faces and closer to the centre,

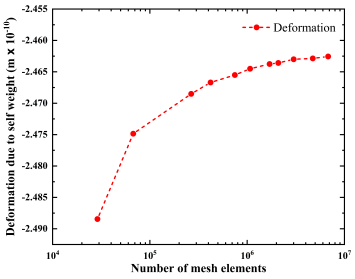

Fig. 5. Study of mesh convergence, where total deformation is plotted as a function of number of mesh elements.

the redistribution of weight causes the outer sections of the cavity to bend more downward. Since the mirror centres move oppositely, this bending results in variation in optical length in the opposite direction. Between these extreme positions, there is an optimal spot where deformation is minimal. This can be identified by finding the zero-crossing point in the plot of fractional deformation along the optical length against the variation in mounting structure positions. This optimal mounting position, where the deformation of the entire body is present, but the displacement of the mirror centres is negligible, is known as the Airy point.

To determine the Airy point position along the axial direction, we varied δz while keeping δx fixed at 18 mm. The zero-crossing point was found at δz ≈ 44.08 mm (shown in Fig. 6). Similarly, by varying δx with δz fixed at 45 mm, the

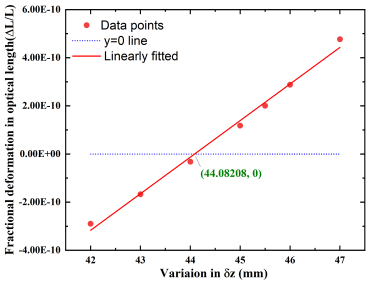

Fig. 6. Simulated result shows a zero crossing in fractional deformation along optical axis at δz ≈ 44.08 mm mm when axial positions (δz) of mounting structures are varied.

zero-crossing point position along the vertical direction was found to be δx ≈ 16.77 mm (shown in Fig. 7). Analysis of these two graphs indicates that achieving a vibration sensitivity on the order of 10^{-11}/g requires machining tolerances within 100μm.

V. Summary and Conclusion

This article primarily addresses the challenges of achieving stability in the optical length of an ultra-stable, high-finesse optical cavity, focusing on issues such as fundamental thermal noise and vibrational noise and methods to mitigate them. We explain how the fundamental thermal noise floor is influenced

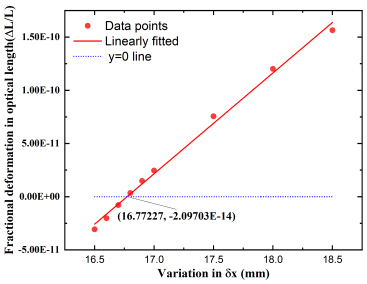

Fig. 7. Simulated result shows a zero crossing in fractional deformation along optical axis at δx ≈ 16.77 mm when positions of mounting structures are varied in along X direction (δx).

by the cavity length and the radius of curvature (ROC) of mirrors, offering insights into optimizing these parameters. The article delves into the use of Finite Element Analysis (FEA) to refine cavity design by examining elastic deformation in the optical length. It highlights the importance of selecting the optimal mesh size and element order in FEA simulations to ensure accurate results. The study emphasizes identifying optimal mounting positions to reduce deformation and achieve lower acceleration sensitivity. Proper mounting, combined with placing the entire setup on an active vibrational isolation floor, can help to attain stability below the expected thermal noise floor for that cavity length.

VI. Acknowledgments

R. Pal gratefully acknowledges financial support from CSIR-UGC (GoI) through the Junior Research Fellowship (JRF) programme. Dr. Arijit Sharma gratefully acknowledges financial support from CAMOST, IIT Tirupati and IIT Tirupati Navavishkar IHUB Foundation. Special thanks to S. Banerjee, J. Yu, C. Ashok, V. Yadav, G. P. Roy, S. Achar, A. Kundu, and H. Miriyala for their valuable inputs and suggestions.

References

[1] E. Boldbaatar, D. Grant, S. Choy, S. Zaminpardaz, and L. Holden, "Evaluating optical clock performance for GNSS positioning," Sensors, vol. 23, pp. 5998, June 2023.

[2] S. De and A. Sharma, "Indigenisation of the Quantum Clock: An Indispensable Tool for Modern Technologies," Atoms, vol. 11, pp. 71, April 2023.

[3] J. Alnis, A. Matveev, N. Kolachevsky, Th. Udem, and T. Hänsch, "Subhertz linewidth diode lasers by stabilization to vibrationally and thermally compensated ultralow-expansion glass Fabry-Perot cavities," Phys. Rev. A, vol. 77, pp. 053809, May 2008.

[4] T. Kessler, T. Legero, U. Sterr, "Thermal noise in optical cavities revisited," J. Opt. Soc. Am. B, vol. 29, pp. 178–184, January 2012.

[5] L. Chen, J.L. Hall, J. Ye, T. Yang, E. Zang, T. Li, "Vibration-induced elastic deformation of Fabry-Perot cavities," Phys. Rev. A, vol. 74, pp. 053801, November 2006.

[6] S. Häfner, S. Herbers, S. Vogt, C. Lisdat, U. Sterr, "Transportable interrogation laser system with an instability of mod σ_y= 3×10^{-16}," Opt. Express, vol. 28, pp. 16407–16416, May 2020.

[7] S. Banerjee, S. Johnson, Y. Vaghasi, K. Palodhi, S. Haldar, S. De, "Modelling and design of ultra-high stable Fabry–Pérot cavity," Int. J. Mech. Sci., vol. 250, pp. 108299, July 2023.

[8] L. Yu, "Internal thermal noise in the ligo test masses: A direct approach," Phys. Rev. D, vol. 57, pp. 659–663, January 1998.